ARTICLE

Seamless Metallic Coating and Surface Adhesion of Self-Assembled Bioinspired Nanostructures Based on Di-(3,4-dihydroxy-L-phenylalanine) Peptide Motif

Galit Fichman,[†] Lihi Adler-Abramovich,[†] Suresh Manohar,[‡] Iris Mironi-Harpaz,[§] Tom Guterman,[†] Dror Seliktar,[§] Phillip B. Messersmith,[‡] and Ehud Gazit[†,⊥,*]

[†]Department of Molecular Microbiology and Biotechnology, George S. Wise Faculty of Life Sciences, Tel Aviv University, Tel Aviv 6997801, Israel, [‡]Biomedical Engineering Department, Northwestern University, Evanston, Illinois 60208, United States, [§]Faculty of Biomedical Engineering, Technion - Israel Institute of Technology, Haifa 32000, Israel, and [⊥]Department of Materials Science and Engineering, Iby and Aladar Fleischman Faculty of Engineering, Tel Aviv University, Tel Aviv 6997801, Israel

ABSTRACT The noncoded aromatic 3,4-dihydroxy-L-phenylalanine (DOPA) amino acid has a pivotal role in the remarkable adhesive properties displayed by marine mussels. These properties have inspired the design of adhesive chemical entities through various synthetic approaches. DOPA-containing bioinspired polymers have a broad functional appeal beyond adhesion due to the diverse chemical interactions presented by the catechol moieties. Here, we harnessed the molecular self-assembly abilities of very short peptide motifs to develop analogous DOPA-containing supramolecular polymers. The DOPA-containing DOPA—DOPA and Fmoc—DOPA—DOPA building blocks were designed by substituting the phenylalanines in the well-studied diphenylalanine self-assembling motif and its 9-fluorenylmethoxycarbonyl (Fmoc)-protected derivative. These peptides self-organized into fibrillar nanoassemblies, displaying high density of catechol functional groups. Furthermore, the Fmoc—DOPA—DOPA peptide was found to act as a low molecular weight hydrogelator, forming self-supporting hydrogel which was rheologically characterized. We studied these assemblies using electron microscopy and explored their applicative potential by examining their ability to spontaneously reduce metal cations into elementary metal. By applying ionic silver to the hydrogel, we observed efficient reduction into silver nanoparticles and the remarkable seamless metallic coating of the assemblies. Similar redox abilities were observed with the DOPA—DOPA assemblies. In an effort to impart adhesiveness to the obtained assemblies, we incorporated lysine (Lys) into the Fmoc—DOPA—DOPA building block. The assemblies of Fmoc—DOPA—DOPA—Lys were capable of gluing together glass surfaces, and their adhesion properties were investigated using atomic force microscopy. Taken together, a class of DOPA-containing self-assembling peptides was designed. These nanoassemblies display unique properties and can serve as multifunctional platforms for various biotechnological applications.

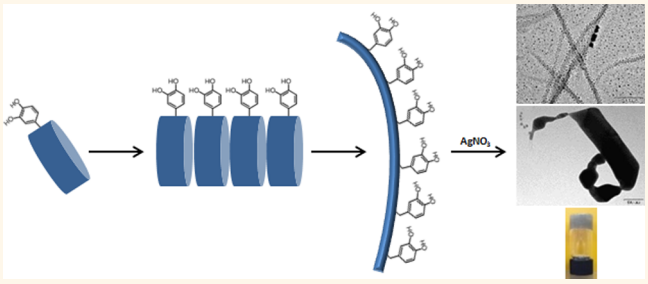

KEYWORDS: self-assembly · peptide nanostructures · supramolecular polymers · metallic coating · bioinspired materials

The phenomenon of bioadhesion provides inspiration for the design of synthetic adhesives in a variety of applications. In recent years, the adhesion of marine mussels has attracted considerable attention due to the unique adhesive properties that these organisms display. Investigations of mussel adhesive proteins (MAPs) have revealed the presence of the noncoded 3,4-dihydroxy-L-phenylalanine (DOPA) aromatic amino acid.[1] Molecular studies on the role of DOPA in these proteins suggested that the catechol moiety has a key role in mussel adhesion.[2−4] Consequently, in the past decade, researchers have applied various synthetic chemistry approaches to form mussel-inspired adhesives by the incorporation of DOPA and other catechol derivatives into natural and synthetic polymers.[5−10] The modification of polymers with catechol groups draws significant attention beyond adhesion due to the abilities of these

* Address correspondence to ehudg@post.tau.ac.il.

Received for review April 23, 2014 and accepted June 17, 2014.

Published online June 17, 2014
10.1021/nn502240r

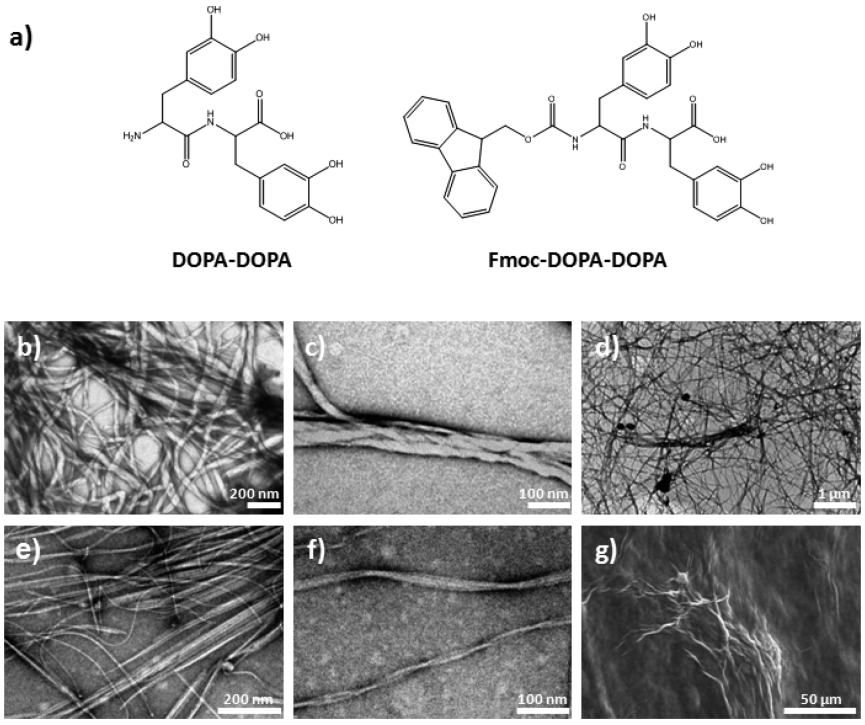

Figure 1. DOPA-containing self-assembling peptides form ordered assemblies. (a) Chemical structure of the DOPA-containing designed peptides. (b,c) TEM micrographs of DOPA–DOPA dipeptide assemblies; (d–f) TEM micrographs of the hydrogel-forming Fmoc–DOPA–DOPA assemblies; (g) E-SEM micrograph of the Fmoc–DOPA–DOPA hydrogel after gradual dehydration.

groups to act as antioxidant agents, radical trappers, metal chelators, oxidizable reducing agents, *etc.*[9,11] Although this approach has been successfully used for various important applications, one major challenge remains: the ability to present a high density of catechol functional groups in a defined supramolecular organization and architecture at the nanoscale. To meet this challenge, we decided to mimic adhesive biological systems by incorporating the DOPA functional groups in self-assembling peptides. Our aim was to harness the molecular self-assembly process to form well-ordered structures endowed with functional properties due to a dense display of catechol moieties. The ability of short aromatic peptides to self-assemble into ordered nanostructures[12,13] and the organization of 9-fluorenylmethoxycarbonyl (Fmoc)-modified peptides into hydrogels of nanoscale order[14−17] motivated us to design short self-assembling building blocks containing DOPA moieties: the DOPA–DOPA and Fmoc–DOPA–DOPA peptides (Figure 1a).

The rationale of the design scheme was based on the aromatic-directed self-assembly of short peptide recognition motifs into ordered structures.[13] The design of the DOPA–DOPA peptide was based on the well-studied diphenylalanine peptide (FF) which self-assembles into discrete nanotubes,[18−21] while the design of Fmoc–DOPA–DOPA-protected dipeptide was based on the well-characterized and biotechnologically utilized low molecular weight (LMW) Fmoc-FF hydrogelator.[15,16,22−26] In these two model peptides, the phenylalanine residues play a key role in the formation of ordered structures through π-stacking and additional noncovalent interactions. From a structural perspective, by substituting the phenylalanine residues with DOPA, we assumed that π-stacking interactions between the aromatic DOPA groups would facilitate molecular recognition and self-assembly, similarly to the interactions of phenylalanine moieties in the well-ordered structures formed by FF.[18] Further support for our assumption is a comprehensive virtual screen of all 400 naturally occurring dipeptides, which revealed the high propensity of aromatic dipeptides to form ordered nanostructures.[13] From an applicative perspective, the design of the peptides stemmed from the assumption that the ordered catecholic groups of DOPA would impart the formed nanostructures with functionally relevant characteristics including adhesiveness, metal ion complexation, and redox activity.

RESULTS AND DISCUSSION

The designed DOPA–DOPA and Fmoc–DOPA–DOPA peptides were examined under different conditions and were found to self-assemble into ordered nanostructures in the presence of ethanol and water (Figure 1b–g). Macroscopically, the Fmoc–DOPA–DOPA peptide formed a self-supporting hydrogel (Figure 2). To gain a better insight into the molecular organization and morphology of the formed structures, electron microscopy was employed. Transmission electron microscopy (TEM) analysis of both peptides

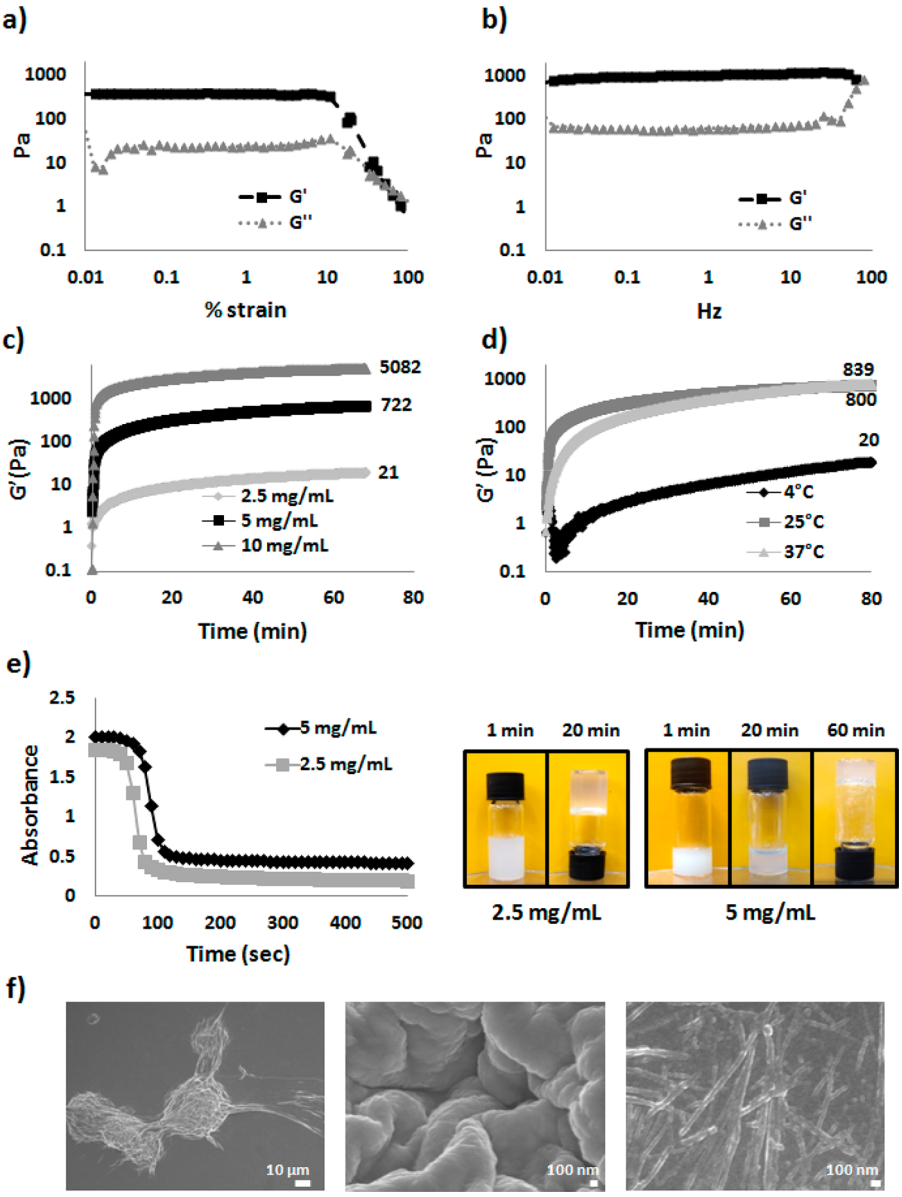

Figure 2. Rheological and structural properties of the Fmoc−DOPA−DOPA hydrogelator. Strain sweep (a) and frequency sweep (b) characterization of 5 mg/mL *in situ*-formed hydrogel at 25 °C. (c) Gelation kinetics of Fmoc−DOPA−DOPA at different concentrations at 25 °C. (d) Gelation kinetics of 5 mg/mL Fmoc−DOPA−DOPA at different temperatures. (e) Kinetics of absorbance at 405 nm at two concentrations and macroscopic visualization of the preparation. (f) HR-SEM micrographs of the turbid peptide solution immediately after inducing the assembly process (left and center panels) and of the semi-transparent gel after 2 h of incubation (right panel).

revealed the formation of a tangled fibrous network composed of flexible, elongated fibrillar structures. We observed the existence of twisted multistrand fibers alongside single fibrils. The DOPA−DOPA dipeptide assembled into fibers with a cross section ranging from 20 to 50 nm (Figure 1b,c), while Fmoc−DOPA−DOPA formed narrower fibers, varying in width from approximately 4 to 30 nm (Figure 1d−f). To characterize the morphology of the Fmoc−DOPA−DOPA hydrogel under humid conditions, environmental scanning electron microscopy (E-SEM) was carried out. Upon gradual dehydration of the sample, a network of supramolecular substructures was observed (Figure 1g).

The hydrogel formed by the LMW Fmoc−DOPA−DOPA peptide was further characterized (Figure 2). The viscoelastic properties of the gel were assessed using rheological measurements. Oscillatory strain (0.01−100%) and frequency sweep (0.01−100 Hz) tests were conducted to determine the linear viscoelastic regime (Figure 2a,b). These tests revealed that, at the linear region, the storage modulus (G') of the hydrogel is more than 1 order of magnitude larger than the loss modulus (G''), a rheological behavior that is characteristic of elastic hydrogels. As shown in Figure 2c, the plateau storage modulus of the hydrogel was found to be modulated with a high dynamic range of ~20 Pa to

~5 kPa, corresponding to the final concentration of the peptide. Furthermore, the gelation kinetics was found to be temperature-dependent (Figure 2d), as gelation was highly decelerated at 4 °C compared to 25 or 37 °C. At higher temperatures (25 or 37 °C), the storage moduli of the hydrogels were approximately 40-fold higher than the storage modulus of hydrogels formed at 4 °C. The gelation process of Fmoc–DOPA–DOPA was also accompanied by a change in the optical properties of the sample, transforming from a turbid viscous solution to a semitransparent hydrogel (Figure 2e). When the 2.5 mg/mL sample was observed macroscopically, the solution cleared within minutes, corresponding to the formation of the hydrogel (Figure 2e). In contrast, in the case of the 5 mg/mL sample, although the solution cleared within minutes, gelation occurred after longer periods of time (Figure 2e). This interesting macroscopic observation is not fully understood; typical self-assembly processes have a higher rate as the concentration increases. This contrasting finding suggests that, at high concentrations, initial disordered aggregation is followed by internal reorganization, which facilitates the subsequent macroscopic transition. This hypothesis is consistent with high-resolution structural examination. High-resolution SEM (HR-SEM) analysis of the 5 mg/mL samples taken minutes or hours after the initiation of the assembly process (Figure 2f) indicated that large aggregates are present at the initial stage when the solution is turbid, whereas after several hours, ordered structures with much smaller diameter appear, corresponding to a considerably clearer solution. This observation is also in line with a previous hypothesis put forward by our group linking the optical transition from turbid to transparent in Fmoc-protected hydrogel preparation to the structural organization over time.[27] This restructuring, from irregular aggregates with dimensions similar to or higher than the wavelengths in the visible spectrum to ordered structures with final diameters much lower than these wavelengths, results in the change of the scattering properties of the solution. It should be mentioned that a similar optical phenomenon was also reported with regards to the hydrogelation process of another LMW Fmoc-containing hydrogelator.[28] The increase in turbidity was explained in light of a phase separation process, leading to the formation of unstable spherical assemblies. The subsequent clearing of the solution and hydrogelation were correlated with the formation of a fibrous network at the expanse of the spherical assemblies.

Following the characterization of DOPA–DOPA and Fmoc–DOPA–DOPA peptides, we decided to explore the functional properties of the catecholic groups and investigate the redox properties of the assemblies by monitoring the reduction of ionic silver. The catechol group of the DOPA residues is redox-active, allowing the spontaneous reduction of metal cations into solid metal.[11] This property was previously utilized to prepare gold and silver nanoparticles from gold chloride or silver nitrate.[29−31] Recently, catechol redox chemistry was also utilized to form polymer-coated metal nanoparticles and mussel-inspired silver-releasing antibacterial hydrogels.[32,33] We decided to follow this approach and examine whether the obtained assemblies can spontaneously reduce ionic silver to silver nanoparticles. In addition, this reaction was used to determine the availability and directionality of the functional DOPA moieties in the assembled structures. DOPA groups that are exposed to the solution are expected to react with ionic silver to form silver nanoparticles or clusters that are detectable by electron microscopy. Moreover, the reduction of silver is accompanied by a change in color due to strong absorbance at approximately 410 nm that can be easily observed macroscopically.

The addition of silver nitrate solution to a preprepared Fmoc–DOPA–DOPA hydrogel led to a change in the hydrogel color from semitransparent to dark brown over a period of several hours to a few days (Figure 3a). UV–vis spectra taken 5 days after silver nitrate was added to the hydrogel revealed an increased absorbance above 300 nm. The broad-band increase in absorption in this area could be due to scattering by silver nanoparticles and DOPA oxidation. It should be noted that this change in color did not occur immediately as reported in other systems;[32,33] instead, the kinetics were rather slow. Two possible mechanisms, perhaps co-occurring, could account for this difference. First, the diffusion rate of ionic silver is much lower at the gel phase compared with the solution phase. Indeed, when gel formation occurred in the presence of ionic silver, significantly faster reduction of silver was observed (data not shown). Second, silver reduction by Fmoc–DOPA–DOPA was performed under acidic pH, with the peptide dissolved in water only (pH 5.5). Under these conditions, the silver reduction potential is lower as compared to similar reactions reported in the literature that were carried out under neutral or alkaline pH. When dissolving the peptide in water with the pH adjusted to neutral (pH 7.0) or alkaline (pH 8.0) using diluted NaOH solution, the rate of reduction was indeed higher (data not shown), due to a higher reduction potential of the silver or to the possible existence of solvent-exposed Fmoc–DOPA–DOPA monomers; such monomers exist in buffered neutral or alkaline solution, in which self-assembly and hydrogelation of the peptide are not observed.

The ionic silver reduction process was further monitored by TEM. We observed a slow, gradual transition from the formation of local silver nanoparticle nuclei to the formation of a continuous silver layer (Figure 3b). Distinct formation of silver nanoparticles was observed after short incubation or at a low concentration of the peptide. Under those conditions, most of the fibrillar network was still not coated. However, after longer incubation at high peptide concentration, seamless

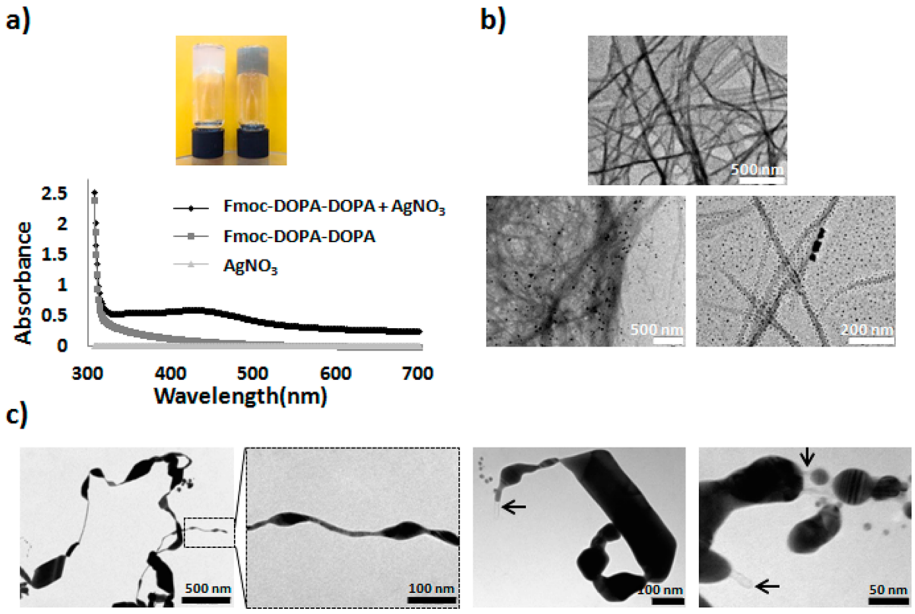

Figure 3. Silver reduction by preprepared Fmoc−DOPA−DOPA hydrogel. (a) Macroscopic visualization and UV−vis spectra of assemblies at 5 mg/mL taken after 5 days of incubation. (b) TEM micrographs of the formation of silver particles after 1 day of incubation of assemblies at 2.5 mg/mL (bottom panels) and a control gel with no addition of silver nitrate (top panel). (c) TEM micrographs of the assemblies at 5 mg/mL after 3 days of incubation. The arrows indicate noncoated peptide assemblies. In all micrographs, negative staining was not applied.

coating of the peptide assemblies was observed in parts of the preparation (Figure 3c). In some cases, we could observe both coated and noncoated areas on the same fibril (Supporting Information Figure S1). Such uniform and continuous coating is unique and is most likely the result of both the slow reduction kinetics as discussed above and the high density of catechol groups presented by the assemblies. Silver reduction was also observed with the addition of ionic silver to DOPA−DOPA peptide assemblies (Figure S2). This redox activity demonstrated by the self-assembling DOPA−DOPA structures could be utilized to produce silver-facilitated antimicrobial materials as well as for additional biotechnological applications.[34−36]

To explore additional functionality, we examined the adhesive properties of the assemblies formed by the two DOPA-containing peptides. Although these assemblies were found to possess inherent redox activity due to their decoration with catechol functional groups, no adhesive properties were macroscopically observable. When considering this finding, it should be noted that the role of DOPA in MAPs and its specific contribution to MAPs adhesion are not fully understood. DOPA could exhibit several adhesion-related functionalities based on the oxidative state of the catechol moiety. The oxidized and non-oxidized catechol functionalities of DOPA are assumed to facilitate cohesion and adhesion of the MAPs, respectively, and it was evident that to a certain extent cohesion is necessary for adhesion.[2] A common belief is that interfacial adhesion to substrates is established by interactions between the non-oxidized catechol form of DOPA and the functional groups at the surface of the solid substrates.[4,37] This may take place given the non-oxidized catechol is able to form (i) hydrogen bonds with hydrophilic polymers, (ii) complexes with metal ions, metal oxide, and silicon dioxide which are all present in mineral surfaces, and (iii) $\pi-\pi$ interactions with aromatic surfaces.[38−41] This chemical interplay clearly complicates any possible interpretation of the lack of adhesive properties presented by the investigated peptides.

Recent evidence suggested that oxidation of DOPA residues to DOPA-quinone or DOPA-semiquinone can lead to intermolecular cross-linking of the MAPs, either with other DOPA residues by a radical mechanism or with the ε-amino group of lysine (Lys) residues by Michael addition mechanism giving rise to solidification of the adhesive.[4] Indeed, lysine is a common residue in MAPs, and the DOPA−Lysine motif was used for the design of adhesive polymers.[42,43]

Due to the suggested significant contribution of the ε-amino group to the cohesive properties, we hypothesized that the incorporation of lysine residues into the DOPA-containing peptide assemblies would contribute to cohesion and thus indirectly improve adhesion. Moreover, lysine residues may also contribute to adhesion *via* ionic bonding to negatively charged surfaces. Therefore, we designed the Fmoc−DOPA−DOPA−Lys-protected tripeptide. Upon examination of the protected tripeptide under the conditions applied to the two peptides studied initially, the Fmoc−DOPA−DOPA−Lys peptide was also found to self-assemble into well-ordered fibrillar structures that show some degree of resemblance to the fibers obtained by Fmoc−DOPA−DOPA (Figure 4a). However, in contrast to the fibers

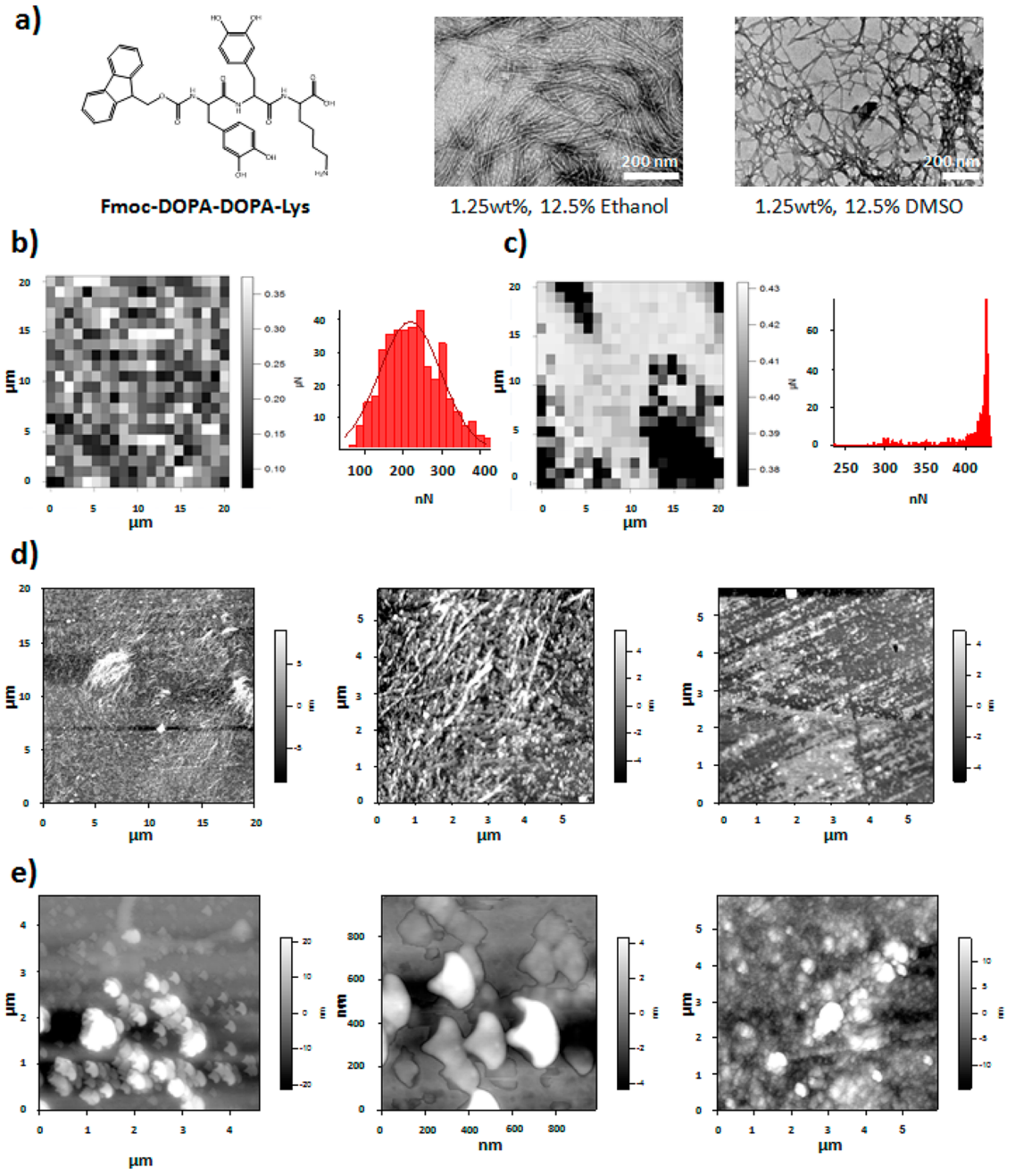

Figure 4. Characterization of Fmoc−DOPA−DOPA−Lys assemblies. (a) Chemical structure and TEM analysis of 1.25 wt % (17.2 mM) Fmoc−DOPA−DOPA−Lys assemblies prepared in either 12.5% ethanol or 12.5% DMSO. (b) Adhesion force map and corresponding histogram of 1.25 wt % Fmoc−DOPA−DOPA−Lys prepared in ethanol and water. (c) Adhesion force map and corresponding histogram of 1.25 wt % Fmoc−DOPA−DOPA−Lys prepared in DMSO and water. (d) AFM images of the exposed area of the bottom (left and center panels) and top (right) glass surfaces after peeling two glass slides that were adhered overnight by an aliquot of 1.25 wt % Fmoc−DOPA−DOPA−Lys in 12.5% ethanol. (e) AFM images of the exposed area of the bottom (left and center panels) and top (right panel) glass surfaces after peeling two glass slides that were adhered overnight by a preparation of 1.25 wt % Fmoc−DOPA−DOPA−Lys in 12.5% DMSO.

formed by the latter, the fibers assembled by the Fmoc−DOPA−DOPA−Lys were narrower, with an approximated width of less than 10 nm. Moreover, the fine fibers were only formed by dissolving the peptide to higher concentrations (1.25 *versus* 0.5 wt %). Fmoc−DOPA−DOPA−Lys was also found to self-assemble into ordered nanostructures in the presence of dimethyl sulfoxide (DMSO) and water, forming assemblies with high structural similarity to the Fmoc−DOPA−DOPA structures (Figure 4a).

Macroscopically, we observed that this tripeptide forms viscoelastic glue capable of adhering two glass slides. To quantify the adhesive forces of the tripeptide sample to the glass surfaces, atomic force microscopy (AFM) was used. Specifically, we assessed the adhesion of the structures to a silicon oxide (SiO_2) colloidal probe

by employing force–distance measurements. This type of measurement allows the determination of the attractive forces between the AFM probe and the contacted surface, where this force is represented by the minimum value of the force–distance curve.[44] To estimate the adhesion of the self-assembled structures to silicon oxide, peptide solution was deposited on a glass slide and several force–distance curves were measured at different locations. We also calculated the average adhesion of the peptides in a broader area by adhesion force maps (Figure 4b,c).

Our results revealed that the examined tripeptide possesses the ability to adhere to silicone oxide, in accordance with our macroscopic observation. In comparison to the very low adhesion of the AFM probe to bare glass, a glass surface covered with Fmoc–DOPA–DOPA–Lys tripeptide assemblies displayed significant adhesive forces (Figure 4b,c). The adhesion of the tip to bare glass was less than 10 nN, whereas adhesion to the Fmoc–DOPA–DOPA–Lys preparation to the glass was calculated to be more than 300 nN when prepared in DMSO and 214 nN (mean force) when prepared in ethanol. To compare the adhesion of the Fmoc–DOPA–DOPA–Lys assemblies to the Fmoc–DOPA–DOPA assemblies, force maps were measured for the latter when prepared in ethanol at the same molar concentration (17.2 mM). The obtained histograms reveal that more counts corresponding to forces above 200 pN were present in the preparation of the protected tripeptide as compared to the dipeptide one (Figure S3). Similar behavior was also observed under lower concentration (12.9 mM, Figure S4).

As noted above, under both ethanol and DMSO conditions, the Fmoc–DOPA–DOPA–Lys sample displayed macroscopic adhesive properties, capable of gluing together two glass slides. It should be noted that this gluing phenomenon, in the presence of DMSO, showed recovery behavior—after separating the glass slides by peeling, they were able to be rejoined. Interestingly, this was not the case when ethanol was used for the preparation of Fmoc–DOPA–DOPA–Lys solutions; when this procedure was repeated with an ethanol-prepared tripeptide sample, the sample lost its adhesive properties after peel forces were applied. To understand the basis for the recovery differences between the DMSO and ethanol tripeptide samples, after the two glass slides were glued together, we peeled off the top glass slide and examined the exposed area. AFM analysis of Fmoc–DOPA–DOPA–Lys in ethanol after peeling exhibited unidirectional fine fibrous structures (Figure 4d). In contrast, AFM analysis of Fmoc–DOPA–DOPA–Lys in DMSO after peeling revealed the presence of twisted spheres that were unidirectionally retracted (Figure 4e). It therefore seems that the existence of the larger patches of peptide assemblies have a role in the re-adhesion process.

CONCLUSIONS

In summary, we have shown that the substitution of phenylalanine with DOPA in the known self-assembling peptide motif FF yields self-assembling peptides that are able to form ordered supramolecular nanostructures substantially decorated with catechol functional groups. Due to the intrinsic properties of the catechol group, the obtained supramolecular structures can be used as multifunctional platforms for various technological applications. Upon the incorporation of additional lysine residue containing ε-amine, significant adhesion was obtained, possibly due to electrostatic interactions between the protonated amine and negatively charged oxide surface. The remarkable seamless silver deposition reflects the tendency of the dense catechol array to facilitate coating rather than adhesion. The properties of this deposition are unique, as compared to any known electroless metal coating of biological or polymer nanoassemblies and should prove very useful in the templating of inorganic materials on organic surfaces at the nanoscale for various applications.

METHODS

Preparation of Peptide Assemblies. All peptides were synthesized by Peptron Inc. (Daejeon, South Korea). The peptides were purified to 96–98%, and their identity was confirmed by mass spectrometry. For the formation of DOPA–DOPA asssemblies, lyophilized peptide was dissolved in ethanol to a concentration of 33 mg/mL then diluted with Milli-Q water to a final concentration of 5 mg/mL. For the formation of Fmoc–DOPA–DOPA assemblies, lyophilized peptide was dissolved in ethanol to a concentration of 100 mg/mL then diluted with Milli-Q water to the desired concentration (2.5, 5, or 10 mg/mL). For formation of Fmoc–DOPA–DOPA–Lys assemblies, lyophilized peptide was dissolved in either ethanol or DMSO to a concentration of 100 mg/mL then diluted with Milli-Q water to a final concentration of 12.5 mg/mL.

TEM. TEM analysis was performed by applying 10 μL samples to 400-mesh copper grids covered by carbon-stabilized Formvar film (Electron Microscopy Science, Fort Washington, PA, USA). The samples were allowed to adsorb for 2 min before excess fluid was blotted off. For samples that were negatively stained, 10 μL of 2% uranyl acetate was then deposited on the grid and allowed to adsorb for 2 min before excess fluid was blotted off. TEM micrographs were recorded using JEOL 1200EX electron microscope (Tokyo, Japan) operating at 80 kV.

E-SEM. E-SEM analysis of 5 mg/mL Fmoc–DOPA–DOPA hydrogel was performed by placing a portion of a pre-prepared hydrogel on a microscope metal stand. Images were taken using Quanta 200 field emission gun (FEG) E-SEM (FEI, Eindhoven, The Netherlands) operating at 10 kV.

Rheology. Rheological measurements for *in situ*-formed Fmoc–DOPA–DOPA hydrogel were performed using an AR-G2 rheometer (TA Instruments, New Castle, DE, USA). Time-sweep oscillatory tests in 20 mm parallel plate geometry were conducted at 0.7% strain and 1 Hz frequency on 200 μL of fresh solution (resulting in a gap size of about 0.6 mm), 1 min after its preparation. In order to determine the linear viscoelastic region, oscillatory strain (0.01–100%) and frequency sweep (0.01–100 Hz) tests were conducted 45 min after diluting the stock solution with

Milli-Q water. All rheology tests were done in triplicate and averaged.

Turbidity Analysis. Turbidity analysis for Fmoc−DOPA−DOPA solutions was conducted using freshly prepared solutions at concentrations of 2.5 and 5 mg/mL. Then, 200 μL aliquots were pipetted into a 96-well plate, and absorbance at 405 nm was measured over time, starting 45 s after the preparation of the peptide solution. All measurements were performed using a Biotek Synergy HT plate reader (Winooski, VT, USA) at 25 °C.

HR-SEM. HR-SEM analysis was done for Fmoc−DOPA−DOPA hydrogels at different time points following the initiation of peptide self-assembly. Then, 10 μL samples were dried at room temperature on microscope glass coverslips and coated with chromium. Images were taken using a JEOL JSM 6700F FE-SEM operating at 10 kV.

Silver Reduction. Silver reduction assay was performed with pre-prepared Fmoc−DOPA−DOPA hydrogels at a concentration of 5 mg/mL (8.35 mM). Then, 50 μL of 13.2 mM silver nitrate was added to 500 μL hydrogel aliquots by gentle pipetting, resulting in 1.2 mM final concentration of silver nitrate. This solution was incubated at room temperature for several days. At different time points, 10 μL aliquots were taken for TEM analysis and negative staining was not applied. To examine silver reduction using UV−vis spectroscopy, silver nitrate was added to a 5 mg/mL hydrogel pre-prepared as described above and 150 μL aliquots of Fmoc−DOPA−DOPA hydrogel with or without silver nitrate were pipetted into a 96-well UV-Star UV transparent plate (Greiner BioOne, Frickenhausen, Germany). Spectra were collected after 5 days using a Biotek Synergy HT plate reader over the range of 300−700 nm and compared to blank samples of silver nitrate only or of the peptide only.

AFM. AFM analysis was performed using Asylum MFP-1D AFM instrument (Asylum Research, Santa Barbara, CA, USA). To obtain force data for Fmoc−DOPA−DOPA−Lys (12.5 mg/mL), samples were prepared in either DMSO or ethanol as described above. After overnight incubation, 10 μL of each sample was deposited on a glass slide and dried at room temperature. Force measurements of the samples were conducted using a SiO_2 colloidal probe (tip velocity 1000 nm/s, compressive force 20 nN).

To investigate the glass surface area morphology after peeling, 30 μL of freshly prepared Fmoc−DOPA−DOPA−Lys solutions (12.5 mg/mL, prepared in DMSO or ethanol as described above) was deposited between two microscope glass slides. This construct was incubated overnight at room temperature under 100 mg weight. Finally, the top glass slide was peeled off and the contact area of either slide was imaged using an Ultrasharp AFM probe (NSC21/Ti−Pt, MikroMasch) operated in tapping mode.

Conflict of Interest: The authors declare no competing financial interest.

Acknowledgment. This work was supported in part by grants from the Israeli National Nanotechnology Initiative and Helmsley Charitable Trust for a Focal Technology Area on Nanomedicines for Personalized Theranostics. G.F. would like to thank the Center for Nanoscience and Nanotechnology at Tel Aviv University, the TAU Global Research & Training Fellowship in Medical and Life Sciences Fund (GRTF), and The Naomi Foundation for travel fellowships. Work in the Messersmith group was supported by Grant R37 DE014193 from the National Institutes of Health. We also thank Z. Barkay for E-SEM analysis, and members of the Gazit and Messersmith laboratories for helpful discussions.

Supporting Information Available: TEM analysis showing partial silver coating of Fmoc-DOPA-DOPA assemblies, HR-SEM analysis and UV-vis spectroscopy demonstrating silver reduction by DOPA−DOPA assemblies, AFM analyses for adhesion comparison between Fmoc-DOPA−DOPA and Fmoc-DOPA−DOPA−Lys assemblies. This material is available free of charge *via* the Internet at http://pubs.acs.org.

REFERENCES AND NOTES

1. Waite, J. H. Adhesion a la Moule. *Integr. Comp. Biol.* **2002**, *42*, 1172–1180.
2. Yu, M. E.; Hwang, J. Y.; Deming, T. J. Role of L-3,4-Dihydroxyphenylalanine in Mussel Adhesive Proteins. *J. Am. Chem. Soc.* **1999**, *121*, 5825–5826.
3. Lee, H.; Scherer, N. F.; Messersmith, P. B. Single-Molecule Mechanics of Mussel Adhesion. *Proc. Natl. Acad. Sci. U.S.A.* **2006**, *103*, 12999–13003.
4. Silverman, H. G.; Roberto, F. F. Understanding Marine Mussel Adhesion. *Mar. Biotechnol.* **2007**, *9*, 661–681.
5. Kastrup, C. J.; Nahrendorf, M.; Figueiredo, J. L.; Lee, H.; Kambhampati, S.; Lee, T.; Cho, S. W.; Gorbatov, R.; Iwamoto, Y.; Dang, T. T.; *et al.* Painting Blood Vessels and Atherosclerotic Plaques with an Adhesive Drug Depot. *Proc. Natl. Acad. Sci. U.S.A.* **2012**, *109*, 21444–21449.
6. Dalsin, J. L.; Hu, B. H.; Lee, B. P.; Messersmith, P. B. Mussel Adhesive Protein Mimetic Polymers for the Preparation of Nonfouling Surfaces. *J. Am. Chem. Soc.* **2003**, *125*, 4253–4258.
7. Brubaker, C. E.; Kissler, H.; Wang, L. J.; Kaufman, D. B.; Messersmith, P. B. Biological Performance of Mussel-Inspired Adhesive in Extrahepatic Islet Transplantation. *Biomaterials* **2010**, *31*, 420–427.
8. Lee, B. P.; Messersmith, P. B.; Israelachvili, J. N.; Waite, J. H. Mussel-Inspired Adhesives and Coatings. *Annu. Rev. Mater. Res.* **2011**, *41*, 99–132.
9. Sedo, J.; Saiz-Poseu, J.; Busque, F.; Ruiz-Molina, D. Catechol-Based Biomimetic Functional Materials. *Adv. Mater.* **2013**, *25*, 653–701.
10. Meredith, H. J.; Jenkins, C. L.; Wilker, J. Enhancing the Adhesion of a Biomimetic Polymer Yields Performance Rivaling Commercial Glues. *Adv. Funct. Mater.* **2014**, *24*, 3259–3267.
11. Faure, E.; Falentin-Daudre, C.; Jerome, C.; Lyskawa, J.; Fournier, D.; Woisel, P.; Detrembleur, C. Catechols as Versatile Platforms in Polymer Chemistry. *Prog. Polym. Sci.* **2013**, *38*, 236–270.
12. Reches, M.; Gazit, E. Molecular Self-Assembly of Peptide Nanostructures: Mechanism of Association and Potential Uses. *Curr. Nanosci.* **2006**, *2*, 105–111.
13. Frederix, P. W. J. M.; Ulijn, R. V.; Hunt, N. T.; Tuttle, T. Virtual Screening for Dipeptide Aggregation: Toward Predictive Tools for Peptide Self-Assembly. *J. Phys. Chem. Lett.* **2011**, *2*, 2380–2384.
14. Zhang, Y.; Gu, H. W.; Yang, Z. M.; Xu, B. Supramolecular Hydrogels Respond to Ligand-Receptor Interaction. *J. Am. Chem. Soc.* **2003**, *125*, 13680–13681.
15. Jayawarna, V.; Ali, M.; Jowitt, T. A.; Miller, A. E.; Saiani, A.; Gough, J. E.; Ulijn, R. V. Nanostructured Hydrogels for Three-Dimensional Cell Culture through Self-Assembly of Fluorenylmethoxycarbonyl-Dipeptides. *Adv. Mater.* **2006**, *18*, 611–614.
16. Mahler, A.; Reches, M.; Rechter, M.; Cohen, S.; Gazit, E. Rigid, Self-Assembled Hydrogel Composed of a Modified Aromatic Dipeptide. *Adv. Mater.* **2006**, *18*, 1365–1370.
17. Fichman, G.; Gazit, E. Self-Assembly of Short Peptides to Form Hydrogels: Design of Building Blocks, Physical Properties and Technological Applications. *Acta Biomater.* **2014**, *10*, 1671–1682.
18. Reches, M.; Gazit, E. Casting Metal Nanowires within Discrete Self-Assembled Peptide Nanotubes. *Science* **2003**, *300*, 625–627.
19. Yan, X. H.; Zhu, P. L.; Li, J. B. Self-Assembly and Application of Diphenylalanine-Based Nanostructures. *Chem. Soc. Rev.* **2010**, *39*, 1877–1890.
20. Sedman, V. L.; Chen, X.; Allen, S.; Roberts, C. J.; Korolkov, V. V.; Tendler, S. J. B. Tuning the Mechanical Properties of Self-Assembled Mixed-Peptide Tubes. *J. Microsc. (Oxford, U. K.)* **2013**, *249*, 165–172.
21. Vasudev, M. C.; Koerner, H.; Singh, K. M.; Partlow, B. P.; Kaplan, D. L.; Gazit, E.; Bunning, T. J.; Naik, R. R. Vertically Aligned Peptide Nanostructures Using Plasma-Enhanced Chemical Vapor Deposition. *Biomacromolecules* **2014**, *15*, 533–540.
22. Liebmann, T.; Rydholm, S.; Akpe, V.; Brismar, H. Self-Assembling Fmoc Dipeptide Hydrogel for *In Situ* 3D Cell Culturing. *BMC Biotechnol.* **2007**, *7*, 88.
23. Smith, A. M.; Williams, R. J.; Tang, C.; Coppo, P.; Collins, R. F.; Turner, M. L.; Saiani, A.; Ulijn, R. V. Fmoc-Diphenylalanine Self Assembles to a Hydrogel *via* a Novel Architecture

Based on $\pi-\pi$ Interlocked β-Sheets. *Adv. Mater.* **2008**, *20*, 37–41.
24. Tang, C.; Smith, A. M.; Collins, R. F.; Ulijn, R. V.; Saiani, A. Fmoc-Diphenylalanine Self-Assembly Mechanism Induces Apparent pK_a Shifts. *Langmuir* **2009**, *25*, 9447–9453.
25. Raeburn, J.; Pont, G.; Chen, L.; Cesbron, Y.; Levy, R.; Adams, D. J. Fmoc-Diphenylalanine Hydrogels: Understanding the Variability in Reported Mechanical Properties. *Soft Matter* **2012**, *8*, 1168–1174.
26. Raeburn, J.; Cardoso, A. Z.; Adams, D. J. The Importance of the Self-Assembly Process to Control Mechanical Properties of Low Molecular Weight Hydrogels. *Chem. Soc. Rev.* **2013**, *42*, 5143–5156.
27. Orbach, R.; Mironi-Harpaz, I.; Adler-Abramovich, L.; Mossou, E.; Mitchell, E. P.; Forsyth, V. T.; Gazit, E.; Seliktar, D. The Rheological and Structural Properties of Fmoc-Peptide-Based Hydrogels: The Effect of Aromatic Molecular Architecture on Self-Assembly and Physical Characteristics. *Langmuir* **2012**, *28*, 2015–2022.
28. Chen, L.; Raeburn, J.; Sutton, S.; Spiller, D. G.; Williams, J.; Sharp, J. S.; Griffiths, P. C.; Heenan, R. K.; King, S. M.; Paul, A.; *et al.* Tuneable Mechanical Properties in Low Molecular Weight Gels. *Soft Matter* **2011**, *7*, 9721–9727.
29. Baron, R.; Zayats, M.; Willner, I. Dopamine-, L-DOPA-, Adrenaline-, and Noradrenaline-Induced Growth of Au Nanoparticles: Assays for the Detection of Neurotransmitters and of Tyrosinase Activity. *Anal. Chem.* **2005**, *77*, 1566–1571.
30. Begum, N. A.; Mondal, S.; Basu, S.; Laskar, R. A.; Mandal, D. Biogenic Synthesis of Au and Ag Nanoparticles Using Aqueous Solutions of Black Tea Leaf Extracts. *Colloids Surf., B* **2009**, *71*, 113–118.
31. Lee, Y.; Park, T. G. Facile Fabrication of Branched Gold Nanoparticles by Reductive Hydroxyphenol Derivatives. *Langmuir* **2011**, *27*, 2965–2971.
32. Black, K. C. L.; Liu, Z. Q.; Messersmith, P. B. Catechol Redox Induced Formation of Metal Core–Polymer Shell Nanoparticles. *Chem. Mater.* **2011**, *23*, 1130–1135.
33. Fullenkamp, D. E.; Rivera, J. G.; Gong, Y. K.; Lau, K. H. A.; He, L. H.; Varshney, R.; Messersmith, P. B. Mussel-Inspired Silver-Releasing Antibacterial Hydrogels. *Biomaterials* **2012**, *33*, 3783–3791.
34. Ma, Y. R.; Niu, H. Y.; Zhang, X. L.; Cai, Y. Q. Colorimetric Detection of Copper Ions in Tap Water during the Synthesis of Silver/Dopamine Nanoparticles. *Chem. Commun.* **2011**, *47*, 12643–12645.
35. Paladini, F.; Meikle, S. T.; Cooper, I. R.; Lacey, J.; Perugini, V.; Santin, M. Silver-Doped Self-Assembling Di-phenylalanine Hydrogels as Wound Dressing Biomaterials. *J. Mater. Sci.: Mater. Med.* **2013**, *24*, 2461–2472.
36. Salome Veiga, A.; Schneider, J. P. Antimicrobial Hydrogels for the Treatment of Infection. *Biopolymers* **2013**, *100*, 637–644.
37. Wiegemann, M. Adhesion in Blue Mussels (*Mytilus edulis*) and Barnacles (Genus *Balanus*): Mechanisms and Technical Applications. *Aquat. Sci.* **2005**, *67*, 166–176.
38. Sever, M. J.; Weisser, J. T.; Monahan, J.; Srinivasan, S.; Wilker, J. J. Metal-Mediated Cross-Linking in the Generation of a Marine-Mussel Adhesive. *Angew. Chem., Int. Ed.* **2004**, *43*, 448–450.
39. Dalsin, J. L.; Lin, L. J.; Tosatti, S.; Voros, J.; Textor, M.; Messersmith, P. B. Protein Resistance of Titanium Oxide Surfaces Modified by Biologically Inspired mPEG-DOPA. *Langmuir* **2005**, *21*, 640–646.
40. Anderson, T. H.; Yu, J.; Estrada, A.; Hammer, M. U.; Waite, J. H.; Israelachvili, J. N. The Contribution of DOPA to Substrate–Peptide Adhesion and Internal Cohesion of Mussel-Inspired Synthetic Peptide Films. *Adv. Funct. Mater.* **2010**, *20*, 4196–4205.
41. Ye, Q.; Zhou, F.; Liu, W. M. Bioinspired Catecholic Chemistry for Surface Modification. *Chem. Soc. Rev.* **2011**, *40*, 4244–4258.
42. Wang, J.; Liu, C. S.; Lu, X.; Yin, M. Co-polypeptides of 3,4-Dihydroxyphenylalanine and L-Lysine To Mimic Marine Adhesive Protein. *Biomaterials* **2007**, *28*, 3456–3468.
43. Yin, M.; Yuan, Y.; Liu, C. S.; Wang, J. Development of Mussel Adhesive Polypeptide Mimics Coating for *In-Situ* Inducing Re-endothelialization of Intravascular Stent Devices. *Biomaterials* **2009**, *30*, 2764–2773.
44. Cappella, B.; Dietler, G. Force–Distance Curves by Atomic Force Microscopy. *Surf. Sci. Rep.* **1999**, *34*, 1–104.